Rheology of dense granular materials: steady, uniform flow and the avalanche regime

2005 J. Phys.: Condens. Matter 17 S2731

(http://iopscience.iop.org/0953-8984/17/24/023)

INSTITUTE OF PHYSICS PUBLISHING JOURNAL OF PHYSICS: CONDENSED MATTER

J. Phys.: Condens. Matter **17** (2005) S2731–S2742 doi:10.1088/0953-8984/17/24/023

Rheology of dense granular materials: steady, uniform flow and the avalanche regime

Jean Rajchenbach[1]

Laboratoire de Physique de la Matière Condensée (CNRS UMR 6622), Université de Nice-Sophia Antipolis, Parc Valrose, 06108 Nice Cedex 02, France

Received 16 March 2005
Published 3 June 2005
Online at stacks.iop.org/JPhysCM/17/S2731

Abstract

In the first part we present experimental results concerning the flow of a densely packed grain collection down a two-dimensional inclined channel. For the range of inclinations corresponding to a steady, uniform regime and to nonsliding conditions at the bottom, we obtain quasi-linear profiles of velocity, that are in contradiction with the predictions of the kinetic theory. We attribute this discrepancy to the inadequacy of the binary collision picture in the case of dense packings. We also show that the various velocity profiles obtained for different flow rates and slopes merge onto a single master curve, according to the following law: $v_X/\sqrt{gd} \propto [\sin(\theta - \theta_c)/\cos\theta_c]^{1/2} y/d$ (d being the grain diameter, θ the channel inclination angle and θ_c the maximal angle of repose), provided that the regime is steady and uniform. Arguing that continuous paths of transient contacts are effective for transporting momentum and energy through the bulk, and that the associated dissipation time is very short compared to the time associated with shearing, we succeed in explaining this scaling behaviour and the paradoxical nonzero shear rate in the vicinity of the free surface. We also show that for dense particulate flows, the dissipation is mainly due to frictional sliding.

In the second part, we emphasize some remarkable features exhibited by dry grain avalanches in laboratory experiments. According to the slope angle, the rear front propagates either upwards or downwards, with velocity approximately equal to the depth averaged velocity of the avalanche. As a counterpart, in both regimes, the velocity magnitude of the head front remains of the order of twice the depth averaged avalanche velocity. We suggest simple elementary mechanisms capable of accounting for these observations. We propose then an analytical modelling aimed at describing the combined processes governing the avalanche expansion. The two solutions that we obtain for the growth regimes and for the avalanche shapes resemble very closely the observations made in the laboratory and in the field.

[1] On leave from: LMDH (CNRS UMR 7603), Université P et M Curie, 75252 Paris Cedex 05, France.

1. Introduction

In order to improve the processing of powders and of particulate materials, commonly used in civil engineering, mining, chemical, pharmaceutics or food industries, or to prevent natural disasters such as avalanches or landslides it is of the utmost interest to gain insight into the rheology of granular materials. Two major features distinguish granular materials from atomic or molecular systems. Firstly, fluctuations of thermal origin are irrelevant, so that the standard route used to derive hydrodynamic equations from equilibrium statistical mechanics and linear response theory must be revisited. Secondly, particles interact via dissipative interactions, namely inelastic collisions and solid friction. Dissipations imply that steady motion states require a permanent forcing. Up to now, most of modellings proceeded from the classical hard sphere gas theory, adapted to account for collisional inelasticity and for friction (Haff 1983, Jenkins and Richman 1985) (for an extensive review see Savage 1993). In such models, collisions are supposed binary, i.e. the medium is supposed dilute enough. In order to map onto the classical kinetic theory, the granular temperature is defined from the velocity fluctuations as $T = \langle v^2 \rangle - \langle v \rangle^2$ (Ogawa *et al* 1980). The mass and momentum balance equations read as usual (because the collisional inelasticity does not intervene in the motion of the centre of mass of a couple of colliding particles). As a counterpart, the inelastic dissipation intervenes in the energy balance. The inelastic energy loss associated with a binary collision reads as $\Delta E = 1/4\, m(1 - e^2)[\mathbf{n_{12}} \cdot (\mathbf{v_1} - \mathbf{v}_2)]^2$, where m is the particle mass, e the inelastic restitution coefficient and $\mathbf{n_{12}}$ the unit vector normal to the collision plane. Since the collision frequency is equal to $T^{1/2}/\lambda$ (λ being the mean free path) and since the typical magnitude of $(v_1 - v_2)^2$ corresponds to the granular temperature, the inelastic energy sink reads as $\Delta E \propto (1 - e^2)T^{3/2}/\lambda$ in the continuum limit (Haff 1983). Equating then the viscous heating to the inelastic energy sink yields the following relation:

$$\dot{\gamma} \propto (1 - e^2)^{1/2} \lambda^{-1} T^{1/2} \tag{1}$$

between the shear rate $\dot{\gamma}$ and the granular temperature and the 'constitutive-like' relation:

$$\sigma \propto (1 - e^2)^{-1/2} \lambda^2 \dot{\gamma}^2 \tag{2}$$

(σ being the shear stress) for simple, isothermal shear flows (here, friction and the subsequent coupling with rotational degrees of freedom are disregarded). The quadratic dependence of the shear stress on the shear rate was first proposed by Bagnold (1954), arguing that for a shear flow of nonthermal particles, both the collisional momentum exchange and the collision rate are proportional to $\dot{\gamma}$. Note that the kinetic theory departs from Bagnold's approach by emphasizing the role of the granular temperature. It is thus necessary to solve the coupled set of conservation equations to obtain spatial information related to density, velocity or temperature fields. It is moreover worth noting that, contrary to the case for a simple fluid, the uniqueness of the steady solution is not ensured for a given set of boundary conditions and that the steady solution may depend of the initial (supply) conditions (Shen and Babic 1999).

We are interested here in the flowing properties of systems constituted of dry, noncohesive collections of grains. From laboratory experiments, it is known that such granular materials can exhibit different kinds of flows according to the magnitude of the supply flux (Rajchenbach 1990). For a large flux, the flow appears to be continuous, in opposition to the case for the regime of weak supply flux for which the flow displays a series of discrete avalanches. The existence of these two different regimes originates in the requirement for the free surface slope to exceed a certain angle θ_{start} to initiate the flow. If the spontaneous discharge rate of the flow is not balanced by the uphill supply flux, the slope progressively decreases and the flow stops at angle θ_{stop}. Then a new avalanche is generated after the delay time required to store enough supply matter and to increase again the slope up to the angle θ_{start}. In contrast, if the supply

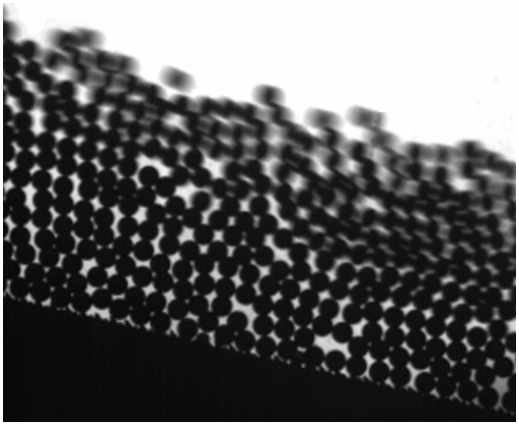

Figure 1. Flow of a collection of monodisperse aluminium spheres (restitution coefficient $e = 0.6$, flow rate $\cong$ 1100 grains s^{-1}, slope angle 21°, exposure time of the photograph: 1/125 s).

flux is equal to or larger than the natural discharge rate of one avalanche, the continuous flow regime is encountered. In the first part, we report recent advances concerning the continuous flow regime of densely packed materials in the inclined channel geometry. Next, we address the particular phenomenon of triggering and expansion of grain avalanches.

2. Flow of a densely packed material down an inclined channel

2.1. Experimental results

So far, there has been a reasonable qualitative agreement between the results of experiments conducted on dilute granular media and the predictions of kinetic models (Azanza *et al* 1999). However, experiments conducted on densely packed media, characterized by the existence of long lasting contacts between grains, lead to drastically different results, results which appear to lie beyond the domain of validity of standard hydrodynamic descriptions. We attribute this discrepancy to the inadequacy of the binary collision picture in the case of densely packed materials. Contrary to the dilute flows case, for which the transport of momentum proceeds from ballistic flights and interparticle collisions, we suggest that in dense flows, the momentum transmission is supported by continuous paths of transient contacts through the bulk.

We have performed experiments in a two-dimensional inclined channel, sloping between 20° and 30°. The bottom is constituted of a saw-blade which ensures nonslipping boundary conditions at the bottom for gentle slopes. The granular material is constituted of monodisperse aluminium spheres of 1.5 mm diameter, with elastic restitution coefficient $e = 0.6$ and friction coefficient $k = 0.6$. The flows are filmed with a digital camera (250 frames s^{-1}) and pictures are then analysed to access grain position and velocity. A typical picture of the flow is shown in figure 1. Corresponding solid fraction and velocity profiles are shown in figure 2. The salient features are the following. Firstly, all grains are in contact with their nearest neighbours, which is far from the picture of a 'granular gas'. The solid fraction appears as nearly constant in the flowing layer (figure 2), with value $\nu \cong 0.8$ corresponding to the random close packing in two dimensions (except for the very top region, owing to the unevenness of the free surface). Secondly, the shear rate $\dot{\gamma}$ is found to be very little dependent on altitude, i.e. the velocity profile looks quasi-linear, and its order of magnitude is given by $\sqrt{g/d}$, where g is the gravity constant and d is the grain diameter. Note that the shear rate is nonzero in the vicinity of

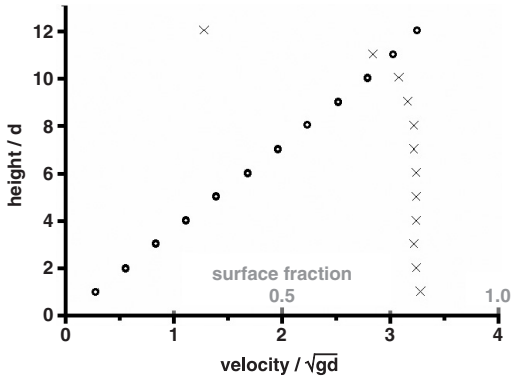

Figure 2. Corresponding adimensioned velocity profile and solid fraction (averaged over 100 samplings).

the free surface, which is paradoxical since the shear stress is zero there. Interestingly, using other materials (such as steel beads), the rheological behaviour is found to be *insensitive* to the value of the restitution coefficient e. Moreover, it is worth noting that particles located in the vicinity of the free surface experience neither saltation nor rebound. The absence of rebound shows that, in such dense assemblies, the effective restitution coefficient is zero whatever its value determined from binary collision experiments. As for the granular temperature, it is important to realize that particle image velocimetry accesses grain displacements only to within the experimental time resolution. In densely packed materials, grains remain in contact, and do not experience free flight punctuated by distinct collisions. Ostensible fluctuations of velocity result actually from the sliding of grains over adjacent corrugated layers of particles.

The above observations are inconsistent with the granular gas theory. According to (1), steady, constant-density, uniformly sheared granular flows are isothermal. In that case, the kinetic theory recovers the Bagnoldian quadratic dependence of the shear stress on shear rate (2) and leads to the following stress balance: $(\partial v_X/\partial z)^2 \propto \rho g z \sin\theta$ (where z is oriented downwards, normal to the flow and x is the direction of the flow) in the steady regime. One therefore obtains $v_X \propto (\rho g h^3 \sin\theta)^{1/2}[1-(z/h)^{3/2}]$ and the 3/2 power law with respect to the depth disagrees with the constant shear rate found experimentally in closely packed media.

2.2. Proposed interpretation

As mentioned above, this discrepancy certainly proceeds from the inadequacy of the binary collision picture in the case of closely packed materials. Collisions of solids involve various phenomena such as deformations, waves, heating (Goldsmith 1960). The *coefficient of restitution* is well defined only for *direct* collisions of *free, unconstrained* spheres—as encountered in dilute gases—and it is improper to extend it to the case of multibody collisions (Ivanov 1997). In the latter case, the apparent coefficient of restitution can be considerably smaller than the one defined from binary collisions. Recently, Falcon *et al* (1998) showed experimentally (in a 1D geometry) that a column of spherical grains, colliding as a whole with a ground wall, displays a bounce height decreasing exponentially as the number of grains in the column is increased. In such multibody collisions, the apparent restitution coefficient is seen to be zero as the number of grains in contact exceeds a threshold value.

At the microscopic scale, a deformation wave propagates through the chains of grains in contact, and experiences partial reflection at contacts and damping. The associated velocity

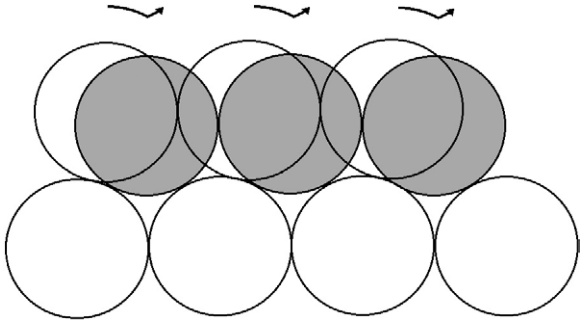

Figure 3. Grain momentum suffers a discontinuity at each impact. The impulsive transfer of momentum has to be taken into account, besides the contact forces in the formulation of the stress tensor.

v_S is that of the sound, typically several hundred metres per second. The passing time of a sound pulse through a grain is given by $\tau_S = d/v_S$, where the sound velocity depends on the confining pressure, owing to the Hertzian stiffness of contacts. For steel beads (with Young modulus $E = 220$ GPa and diameter 8 mm), τ_S ranges from 4 to 8 μs for a confining pressure varied from 0.02 to 2 MPa (Coste and Gilles 1999). The time τ_S must be compared to the time $\dot{\gamma}^{-1}$ (typically 0.1 s) separating two successive collisions suffered by a grain and imposed by the macroscopic shear rate in gravity flow experiments. One can therefore realize that the fastest and most efficient channel for the long range transport of momentum and energy in dense media is associated with sound waves, not with momentum scattering due to distinct collisions, unlike in dilute media. The absence of saltation or rebound results from the damping suffered by momentum and energy during their transport along continuous paths of contacts. The associated dissipation time is of the order of some hundred microseconds (i.e., considerably smaller than the shearing time $\dot{\gamma}^{-1}$) (Falcon *et al* 1998).

Hence, taking into account multibody collisions and the subsequent decrease to zero of the apparent restitution coefficient appears crucial to explaining the rheology of densely packed flow. We emphasize the necessity of giving up the picture of binary collisions, which is at the foundation of the granular gas kinetic theory, in the case of dense packings. In order to establish the motion equations, we adopt here a heuristic approach. We just assume in the following that the damping time is very short compared to $\dot{\gamma}^{-1}$.

In the limit of quasi-static deformations, the stress tensor in densely packed materials can be defined as a function of the set of contact forces. According to Christoffersen *et al* (1981), the static component of the stress tensor reads as $\boldsymbol{\sigma} = (1/2V) \sum_{\text{grains } i \neq j} \mathbf{f}_{ij} \otimes \mathbf{r}_{ij}$, where f_{ij} is the force exerted on grain i by grain j and r_{ij} is the vector from the centroid of grain i to that of grain j (but other definitions can be envisaged). The above term is relevant for describing the regime of very slow deformations accounted for by the (rate-independent) Coulomb plasticity (and the ratio $\sigma_{xy}/\sigma_{yy} = \tan\theta_c$ defines the static angle of friction θ_c). As pointed out by Goddard (1998), for nonzero shear rate, it is necessary to regard the impulsive transfers of momentum between grains besides the contact force network in the equation of motion. Such impulsive transfers of momentum generate a clearly audible acoustic emission, and lead to momentum discontinuities at a frequency $\dot{\gamma}$ (see figure 3). Taking the effective restitution coefficient equal to zero, the momentum discontinuity is proportional to $md\dot{\gamma}$ (where m is the grain mass), so that this mechanism gives rise to a rate-dependent extra term

$$\left.\frac{\mathrm{D}v_x}{\mathrm{D}t}\right|_{\text{coll.}} \propto -d\dot{\gamma}^2 \tag{3}$$

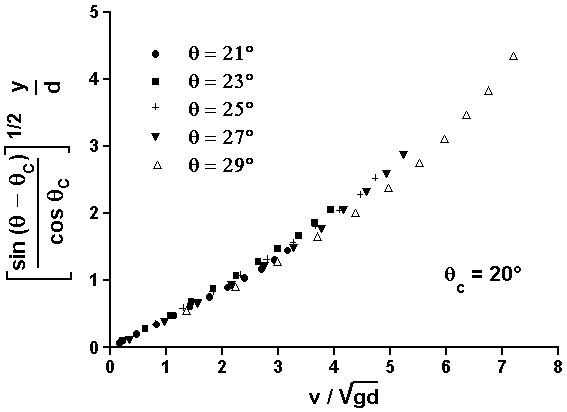

Figure 4. $[\sin(\theta - \theta_c)/\cos\theta_c]^{1/2}(y/d)$ as a function of the dimensionless velocity $v_X/\sqrt{gd}$ for various inclination angles θ ($21° \leqslant \theta \leqslant 29°$). Particles are aluminium spheres (with 1.5 mm diameter). For $\theta = 29°$, the flow is nonuniform and accelerates along the channel.

in the momentum equation (written here per unit mass), $\mathrm{D}/\mathrm{D}t$ being the material derivative. Note that the last term differs from the usual Bagnoldian term

$$\left.\frac{\mathrm{D}v_x}{\mathrm{D}t}\right|_{\mathrm{Bagnold}} \propto -d^2\frac{\partial(\dot\gamma^2)}{\partial z} \tag{4}$$

resulting from binary collisions and corresponding to the viscous stress in a granular gas. One can note one order of difference in the derivatives of the right-hand side of equations (3) and (4). The reason for this dissimilarity is the following. In the kinetic theory, or in Bagnold's model, momentum is hydrodynamically conserved. In contrast, in dense packings, grains are constrained to multiple contacts and the momentum conservation in the centre of mass frame of couples of particles involved in nominal binary collisions is broken.

Adding in equation (3) both gravity and Coulombic friction terms leads to the following equation:

$$\frac{\mathrm{D}v_x}{\mathrm{D}t} = g\sin\theta - g\tan\theta_c - d\left(\frac{\partial v_x}{\partial z}\right)^2 \tag{5}$$

for a dense gravity flow down an incline of slope angle θ (where $\mathrm{D}/\mathrm{D}t$ is the material derivative), from which we derive the following steady solution for the shear rate:

$$\frac{\partial v_x}{\partial y} \propto \left[\frac{\sin(\theta - \theta_c)}{\cos\theta_c}\right]^{1/2}\sqrt{\frac{g}{d}}. \tag{6}$$

The above reasoning predicts a linear velocity profile, that is in fair agreement with the experimental data obtained in the inclined channel geometry for slope angles close to the angle of repose θ_c, and also in the rotating drum set-up (see Nakagawa *et al* 1993, Rajchenbach *et al* 1995, Orpe and Khakhar 2001). This approach succeeds moreover in accounting for the paradoxical nonzero shear rate evidenced in the vicinity of the free surface. Note that equation (6) was previously postulated by Orpe and Khakhar (2001) from analyses of experiments carried out on a rotating drum.

In figure 4, we plot a parameter combining the dimensionless altitude y/d and the following function of the slope: $[\sin(\theta - \theta_c)/\cos\theta_c]^{1/2}$ as a function of the dimensionless velocity $v_X/\sqrt{gd}$, for different inclination angles $21° \leqslant \theta \leqslant 29°$. We can notice that $\dot\gamma$ clearly depends on $[\sin(\theta - \theta_c)/\cos\theta_c]^{1/2}\sqrt{g/d}$ (for $21° \leqslant \theta \leqslant 27°$) and that the linearity of the

velocity profiles improves as θ approaches θ_c. For steeper slopes ($\theta \geqslant 29°$), the flow appears nonuniform and accelerates along the channel (1 m long) and the experimental points do not merge onto the master curve. However, in the last case ($\theta = 29°$) the shear rate remains nonzero in the vicinity of the free surface, unlike in kinetic theory.

The previous result can be extended to polydisperse collections of grains, provided that the segregation phenomenon is accounted for. For the sake of simplicity, consider two species of grains, respectively of diameter d_1 and d_2 ($d_1 > d_2$). In gravity driven flows, the larger species rise up (Savage and Lun 1988), so that, in a rough description supposing a complete demixing, the upper layer constituted of the larger grains displays a shear rate $\dot{\gamma}_1 \propto \sqrt{g/d_1}$ while the lower layer displays a shear rate $\dot{\gamma}_2 \propto \sqrt{g/d_2}$. We can hence deduce that segregation probably induces convexity in the velocity profile of polydisperse flows.

It is of interest to compare the frictional sliding losses to the total dissipation in the inclined channel geometry. In the continuum description, the frictional work reads as $W_f = \int \sigma_{xy} \frac{\partial v_x}{\partial y} \, dV$ (where $\sigma_{xy}/\sigma_{yy} = \tan\theta_c$). In the steady regime, the total dissipation is equal to the decrease of the potential energy $\Delta E_p = \int \rho g \sin\theta \, v_x \, dV$. For such dense flows, the volume fraction is close to that of the random close packing and approximately constant (see figure 2), so that one gets $W_f \approx \int (\tan\theta_c)\sigma_{yy} \frac{\partial v}{\partial y} \, dV = \rho g \cos\theta \tan\theta_c \int v_x \, dV$. We can deduce the ratio of frictional to total dissipation $W_f/\Delta E_p \approx \tan\theta_c/\tan\theta$. For realistic values of θ_c ($\tan\theta_c \cong 20°$ for ballotini, $\tan\theta_c \cong 35°$ for sand) and for $\theta = \theta_c + 5°$, one can estimate that about 80% of the total dissipation proceeds from frictional sliding (Rajchenbach 2003).

The viscous mechanism associated with free flights and collisions is certainly relevant to the case of dilute flows, but it proves inadequate for describing densely packed flows. The above result gives a foundation to the approaches which only consider dry friction in the depth averaged (*à la 'Saint-Venant'*) momentum equation for modelling soil slidings (Savage and Hutter 1989). This approximation is of current use in the geological, geophysical and soil mechanical communities and is of great interest for describing the inertial regime. Nevertheless, Coulomb friction being rate independent, it is necessary to take into account the inelastic dissipation to describe correctly the regime of limiting velocity.

3. Nucleation and growth of grain avalanches

3.1. The two regimes of growth

We address now the issue of the avalanche triggering and of the development in time. First, it is necessary to recall some experimental features, which are at the basis of our analytical description. Two regimes of growth can be distinguished, according to the slope angle (Daerr and Douady 1999). For spontaneous avalanches, starting in the vicinity of the maximum angle of repose θ_{start} (regime I), the rear front propagates up the slope with a velocity $|v\uparrow| \approx |\bar{v}|$, where $\bar{v}$ is the depth averaged velocity of the avalanche (see figure 5) (Rajchenbach 1997, 2002a). In contrast, for avalanches triggered externally (e.g. by perturbing the free surface with a probe) in the range of metastability $\theta_{stop} < \theta < \theta_{start}$ (regime II) the rear front propagates downwards with a velocity approximately equal to $\bar{v}$ (figure 6).

We can advance a simple explanation for this change of behaviour. For $\theta \cong \theta_{start}$, all grains are on the verge of instability, and the first starting grains lead to a series of successive destabilizations upwards. This upwards propagating front corresponds to the onset of motion of particles leaning on neighbouring starting grains down the slope. A simple mass conservation argument allows one to recover the magnitude of the upwards front velocity in regime I. The source term feeding up the avalanche flow rate is related to the advance of the destabilizing front uphill. We get thus $|v\uparrow| \approx \bar{v}$ (where $\bar{v}$ is the depth averaged velocity of the avalanche)

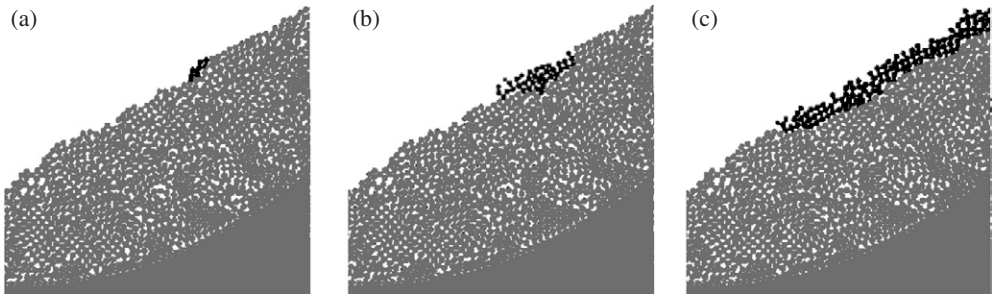

Figure 5. Sequence of pictures showing the nucleation and the propagation of a spontaneous avalanche in regime I. Moving grains are tagged in black. The delay time between snapshots is 0.1 s. In (a), the most unstable particle (or block of particles) is first destabilized. Next ((b) and (c)) we observe the propagation of a kinematic wave uphill, which corresponds to destabilization of uphill adjacent particles leaning on the previous starting grains. Simultaneously, adjacent downhill particles at rest undergo shocks from the head granular jump, triggering their motion.

Figure 6. Sequence of pictures showing the development of an externally triggered avalanche (regime II). The rear front propagates downwards with a velocity equal to the depth averaged velocity $\bar{v}$ of the avalanche. The velocity $v\downarrow$ of the head front is approximately equal to $2\bar{v}$.

because the volume fractions in the frozen and flowing phases are comparable. In contrast, for $\theta_{\rm stop} < \theta < \theta_{\rm start}$, the first falling grains are not able to induce such sequential destabilizations up the slope. Consequently the first starting grains form the rear limit of the avalanche, and rapidly attain their limiting velocity (of the order of $\sqrt{gd}$). To sum up, the rear front velocity displays an abrupt discontinuity (of amplitude $2\bar{v}$) and a change of sign at slope $\theta_{\rm start}$. This analytical singularity can be considered as the proper signature of $\theta_{\rm start}$ and has been clearly evidenced experimentally by Daerr (2001). On the other hand, in both regimes I and II, the head front propagates downwards with a velocity noticeably larger than the depth averaged velocity of the avalanche. The reason is that blocks of grains lying at rest downstream experience destabilizing collisions from the avalanche head front. So the jump is intermittently refreshed, and made up of new grains just entering into motion. More precisely, the velocity $v\downarrow$ of the head front is approximately equal to twice the depth averaged avalanche velocity $\bar{v}$. A look at a microscopic scale shed light on this property. When a block of grains is destabilized as a whole, the head front suddenly advances over a length corresponding to the block size.

Complementarily, between two successive block destabilization events, the front advances with the average avalanche velocity $\bar{v}$ over a distance which compares with the average block size λ. So, the delay time between two destabilization events reads $\tau = \lambda/\bar{v}$, and the time averaged head front velocity is equal to $v\downarrow \widetilde{=} \bar{v} + \lambda/\tau \widetilde{=} 2\bar{v}$ (Rajchenbach 1997, 2002b).

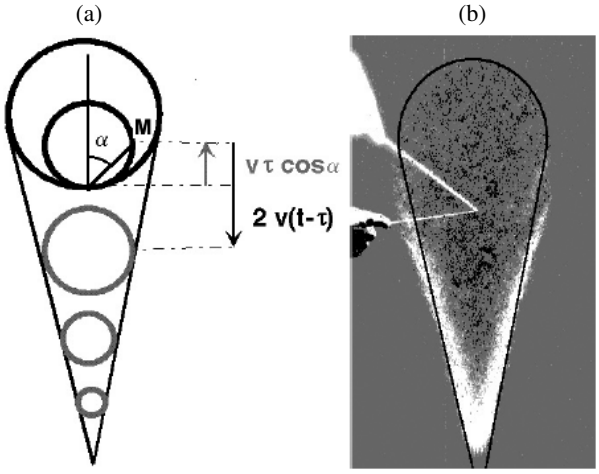

Figure 7. (a) Sketch showing the avalanche growth in the case of spontaneous triggering (regime I; $\theta \approx \theta_{\text{start}}$). According to our modelling, the avalanche area at time t is up of the superimposition of the set of circles of the equation $x^2 + (y + \frac{1}{2}\bar{v}\tau)^2 = (\frac{1}{2}\bar{v}\tau)^2$ shifted down by a length $2\bar{v}(t - \tau)$. (b) Real picture taken by Daerr and Douady (1999).

3.2. Modelling of avalanche growth in three dimensions

3.2.1. Development of spontaneous avalanches (regime I). We propose now to generalize these results issuing from experiments conducted in a two-dimensional configuration to a three-dimensional inclined plane geometry, and to compare our findings with the experimental results reported by Daerr and Douady (1999). The incline is tilted by angle θ with respect to the horizontal. We define the axis Ox as oriented horizontally along the plane, and the axis Oy as oriented downwards along the steepest slope. First consider the upward motion of the rear front. We expect the rear front to propagate along the direction OM, defined by the polar angle $(\text{O}y, \text{OM}) = \pi - \alpha$, with a velocity $|v\uparrow| = \bar{v}\cos\alpha$. The hodograph $v\uparrow(\alpha)$ is therefore a circle. We can write for the loci (x, y) of the rear front at time τ the expression $x^2 + (y + \frac{1}{2}\bar{v}\tau)^2 = (\frac{1}{2}\bar{v}\tau)^2$.

So, the successive positions of the upper boundaries constitute a set of circles passing through the initial point of the avalanche nucleation and with radius increasing linearly in time. It is reasonable to assume then that all grains, once destabilized, fall along the steepest slope direction. Recalling that the avalanche (at time τ) is constituted of all grains destabilized previously during the time interval $[0, \tau]$, and that the lower front propagates with velocity $2\bar{v}$, the avalanche area at time t is constituted by the superimposition of the previous set of circles (labelled for each time τ, $0 < \tau < t$) shifted down by a length $2\bar{v}(t - \tau)$. The equation of this family of circles reads

$$x^2 + \left(y - 2\bar{v}t + \tfrac{5}{2}\bar{v}\tau\right)^2 = \left(\tfrac{1}{2}\bar{v}\tau\right)^2 \qquad 0 < \tau < t. \tag{7}$$

In figure 7(a) we report the family of circles corresponding to equation (1) (in grey). It is easy to recognize the intersection at the tip with angle equal to $2\sin^{-1}\frac{1}{5} \approx 23°$. In figure 7(b) we compare the avalanche boundary determined within this description with an experimental view obtained by Daerr and Douady in the same inclined plane geometry (Daerr and Douady 1999). The agreement is fairly good. Nevertheless we can notice some light differences. The real head front is rounded, while the previous scheme predicts a tip with angle 23°. Three extra mechanisms can be envisaged to explain this rounding effect. Firstly we can consider that

there is a waiting time before the front attains its limiting velocity, so that the actual position of the front is behind the position predicted by this approach which neglects any transient. Secondly we can consider that the grain falls along the steepest slope are accompanied with lateral fluctuating motions, owing to the roughness of the interface. These random motions along the axis Ox can be described by a diffusive mechanism (Samson *et al* 1998), with a diffusion constant $D_\perp = \langle x^2 \rangle / 2t$. Lastly we can consider that the local steepest slope is not actually oriented downwards, because the avalanche forms a bulge and grains tend to be laterally deflected towards the outer edge of the flowing bulge. Let us define the x-component magnitude of the velocity corresponding to the deflection as $v_\perp$. We expect the deflection effect to become more effective at long time than the diffusion, because the deflection leads to a lateral expansion linear in time, whereas the diffusion spread acts like $t^{1/2}$. Nevertheless, note that we previously succeeded in describing the lateral expansion of the avalanche satisfactorily (see figure 7) without taking into account such lateral deflection; this shows that $v_\perp < \bar{v}$.

3.2.2. Development of externally triggered avalanches (regime II). We can also propose an analytical formulation for the growth of externally triggered avalanches, which develop in the range of stability $\theta_{\mathrm{stop}} < \theta < \theta_{\mathrm{start}}$. Since the velocity of the rear front is $\bar{v}$ and that of the head front is $2\bar{v}$, the centre of mass of the avalanche moves downwards with velocity $\frac{3}{2}\bar{v}$. For the sake of simplicity we assume then that the avalanche velocity (referred to in the centre of mass frame) varies continuously from $v_\perp$ (in the Ox-direction) to $\frac{3}{2}\bar{v}$ (in the Oy-direction), according to an elliptic hodograph. Hence, the equation of the avalanche contour at time t can be written parametrically as

$$\left(\frac{\bar{v}x}{2v_\perp}\right)^2 + \left(y - \frac{3}{2}\bar{v}t\right)^2 = \left(\frac{1}{2}\bar{v}t\right)^2. \tag{8}$$

The avalanche track is therefore constituted by the superimposition of homothetic ellipses dilating linearly in time and shifted down by a length $\frac{3}{2}\bar{v}$. It is easy to find that the upper contour of the track is bounded by two straight lines intersecting at the initial locus of the avalanche nucleation with an angle equal to $2\tan^{-1}\frac{2v_\perp}{\sqrt{8}\bar{v}}$. Figure 8 reports the shape of the avalanche track determined according to this modelling. We also show for comparison the real photograph obtained by Daerr and Douady in their experiment dealing with this second category of avalanche morphology (Daerr and Douady 1999). The agreement is very satisfactory. The adjustment of the lateral expansion with time provides the magnitude of the x-component of the velocity: we find $0.10\bar{v} < v_\perp < 0.15\bar{v}$.

3.3. Discussion

It is worth noting that equation (6) is that of a cone which can be considered as the characteristic surface of the following equation:

$$\left(\frac{\partial}{\partial t} + V\frac{\partial}{\partial y}\right)^2 F(x, y, t) = c^2\nabla^2 F(x, y, t) \tag{9}$$

appropriate for describing waves propagating isotropically with speed c and emitted by a source positioned in a moving flow advected with velocity V. For the first avalanche morphology ($\theta \cong \theta_{\mathrm{start}}$), the identification of V with $\frac{5}{2}\bar{v}$ and of c with $\bar{v}/2$ proceeds straightforwardly from equation (1). Hence, the lower boundary of the avalanche identifies with the Mach cone (here in two dimensions), and our modelling brings out an analogy between the avalanche shape and a supersonic wavefront. Regarding the track of the avalanches of the second type ($\theta < \theta_{\mathrm{start}}$), making such an analogy is also possible under the condition of changing the scale of x to

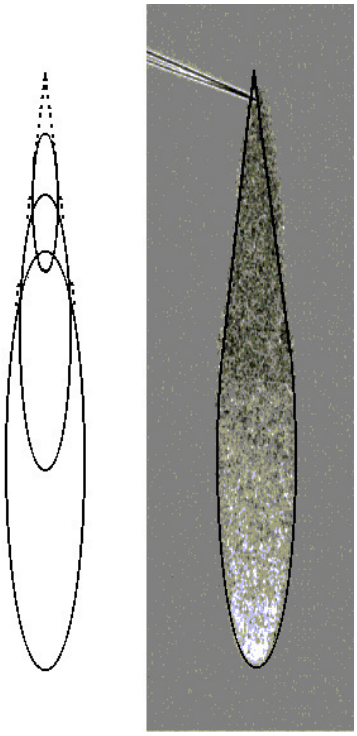

Figure 8. Left: avalanche track at time t (regime of externally triggered avalanches, $\theta < \theta_{\text{start}}$) according to the present modelling. Right: real picture taken by Daerr and Douady (1999).

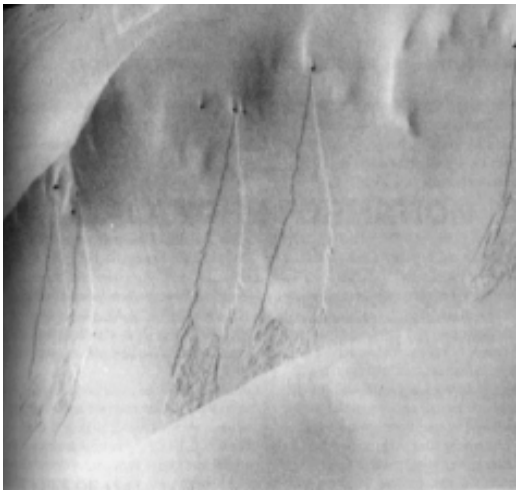

Figure 9. Tracks of loose snow avalanches (photograph taken by Roch, from McClung and Schaerer (1993)).

$x' = (\bar{v}/2v_\perp)x$ in order to reintroduce isotropy. In that case we obtain $V = \frac{3}{2}\bar{v}$ and the Mach cone is oriented upwards.

In figure 9 we show a picture taken by the Swiss Alpinist André Roch (from McClung and Schaerer 1993). This photograph depicts the typical shape of loose snow avalanches.

Surprisingly, although snow is a wet and cohesive material, we recognize a triangular tip oriented upwards, very similar to that exhibited by dry grain avalanches in regime II, and with comparable angle.

Acknowledgments

I acknowledge F Chevoir, A Daerr, J D Goddard, J J Moreau and F Radjai for fruitful discussions.

References

Azanza E, Chevoir F and Moucheront P 1999 *J. Fluid Mech.* **400** 199
Bagnold R G 1954 *Proc. R. Soc.* A **255** 49
Christoffersen J, Mehrabadi M and Nemat-Nasser C 1981 *J. Appl. Mech.* **48** 339
Coste C and Gilles B 1999 *Eur. Phys. J.* B **7** 155
Daerr A 2001 *Phys. Fluids* **13** 2115
Daerr A and Douady S 1999 *Nature* **399** 241
Falcon E, Laroche C, Fauve S and Coste C 1998 *Eur. Phys. J.* B **5** 111
Goddard J D 1998 *Physics of Dry Granular Media* ed H Herrmann, J P Hovi and S Luding (Dordrecht: Kluwer–Academic) p 1
Goldsmith W 1960 *Impact* (London: Edward Arnold)
Haff P K 1983 *J. Fluid Mech.* **134** 401
Ivanov A P 1997 *J. Appl. Math. Mech.* **61** 342
Jenkins J T and Richman M W 1985 *Phys. Fluids* **28** 3485
McClung D and Schaerer P 1993 *The Avalanche Handbook* (Seattle: The Mountaineers Publisher)
Nakagawa M, Altobelli S A, Caprihan A, Fukushima E and Jeong E K 1993 *Exp. Fluids* **16** 54
Ogawa S, Uememura A and Oshima N 1980 *J. Appl. Math. Phys.* **31** 483
Orpe D V and Khakhar A V 2001 *Phys. Rev.* E **64** 031202
Rajchenbach J 1990 *Phys. Rev. Lett.* **65** 2221
Rajchenbach J 1997 *Physics of Dry Granular Media* ed H Herrmann, J P Hovi and S Luding (Dordrecht: Kluwer–Academic) p 421
Rajchenbach J 2002a *Phys. Rev. Lett.* **88** 014301
Rajchenbach J 2002b *Phys. Rev. Lett.* **88** 074301
Rajchenbach J 2003 *Phys. Rev. Lett.* **90** 144302
Rajchenbach J, Clément E and Duran J 1995 *Fractal Aspects of Materials* (*MRS Symposium* vol 367) ed F Family, P Meakin, B Sapoval and R Wool (Pittsburgh, PA: Materials Research Society) p 525
Samson L, Ippolito I, Batrouni G C and Lemaistre J 1998 *Eur. Phys. J.* B **3** 337
Savage S B 1993 *Continuum Mechanics in Environmental Sciences and Geophysics* ed K Hutter (Berlin: Springer) p 467
Savage S B and Hutter K 1989 *J. Fluid Mech.* **199** 177
Savage S B and Lun C K K 1988 *J. Fluid. Mech.* **189** 311
Shen H H and Babic M 1999 *Mechanics of Granular Materials* ed M Oda and K Iwashita (Rotterdam: Balkema) chapter 5